Rubble Detection from VHR Aerial Imagery Data Using Differential Morphological Profiles

G.K. Ouzounis*, P. Soille, M. Pesaresi

Geo-Spatial Information Analysis for Global Security and Stability, Global Security and Crisis Management Unit,
Joint Research Centre, European Commission, Via E.Fermi 2747, I-21027 Ispra (VA), Italy
(georgios.ouzounis, pierre.soille, martino.pesaresi)@jrc.ec.europa.eu

Abstract – Rubble detection is a key element in post disaster crisis assessment and response procedures. In this paper we present an automated method for rapid detection and quantification of rubble from very high resolution (VHR) aerial imagery of urban regions. It is a two step procedure in which the input image is projected onto a hierarchical representation structure for efficient mining and decomposition. Image features matching the geometric and chromatic properties of rubble are fused into a rubble layer that can be re-adjusted interactively. The targeted objects are evaluated based on a density metric given by spatial aggregation. The method is tested on a small-scale exercise on the publicly available aerial imagery of Port-au-Prince, Haiti. Performance and preliminary results are discussed.

Keywords: Rubble detection, earthquake, differential area profile, spatial aggregation.

1. INTRODUCTION

The presence of rubble in urban areas can be used as an indicator of building quality, poverty level, commercial activity, and others. In the case of armed conflict or natural disasters, rubble is seen as the trace of the event on the affected area. The amount of rubble and its density are two important attributes for measuring the severity of the event, in contribution to the overall crisis assessment. In the post-disaster time scale, accurate mapping of rubble in relation to the building type and location is of critical importance in allocating response teams and relief resources immediately after event. In the longer run, this information is used for post-disaster needs assessment (PDNA), recovery planning and other relief activities on the affected region. An example on the 2010 Haiti earthquake is available in (JRC,2010).

Rubble is defined as the remains of building structures, i.e. fragments of irregular size, shape and texture. In remote sensing imagery, aerial or satellite, areas containing rubble are characterized by high intensity variability. Building fragments are usually compact, and of small size that varies depending on the building material, construction quality, and the intensity of the event that generated them. They rest within a small distance from the collapsed structure and their density is a multi-purpose measure for evaluating the extent of the physical damage, the regional accessibility, the risk or cost in human lives, etc. Compiling this rubble characterization and measuring needs, a rubble detection (RD) system is presented based on remote sensing imagery. The RD system targets small size, compact features, both bright and dark, in highly textured VHR images. Full operation cycles on selected image tiles, of the highest scene complexity, suggest that the proposed method can provide reliable results for all stages of post-disaster crisis response.

2. RUBBLE DETECTION SYSTEM

2.1 System Overview

The RD system is based on a modular architecture that allows the customization of the process flow depending on the crisis scenario. It operates on panchromatic images of maximum intensity resolution up to 16 bits/pixel. The system input supports additional geo-referenced sources such as the infrared channel of multi-spectral acquisitions, manually generated masks, digital elevation models (DEM), and others. Pre-disaster VHR imagery can be utilized if available, to extract the building footprints. Rubble-like structures are confirmed as rubble if detected in the vicinity of a building footprint and rejected otherwise. Rubble detected in the pre-disaster acquisition is ignored in the post-disaster process flow. The RD system, following data preparation computes an image representation structure. Image information mining and meta-processes are operated directly on this structure.

2.2 Image Representation

The task of this module is to transfer the image information from the definition domain to some hierarchical representation structure for indexing and fast component retrieval. The current system supports the Max-Tree (Salembier,1998) and α-Tree (Ouzounis,2011b) structures but can easily be adopted to utilize others. The process-flow described, employs the Max-Tree structure which was originally introduced in the context of anti-extensive attribute filtering (Breen,1996). The Max-Tree is a rooted, uni-directed tree in which, nodes correspond to sets of image flat-zones. For each set of flat zones there exists a unique mapping to a peak component. Given a gray-level image f and a level h, a flat-zone is an iso-intensity component at level h of path-connected elements of f, and a peak component is a connected component of the corresponding threshold set at h. The tree node ordering corresponds to the respective peak component nesting; each node points to its parent and the root, corresponding to the set of elements that define the background, points to itself. The leaves of the tree are regional maxima, i.e. flat zones with neighbors of strictly lower intensity. Each Max-Tree node is assigned a unique id which is derived from the image histogram. It is addressed with respect to its level h and node-at-level index k. The node structure consists of 4 primary members but may include others, custom to specific tree operations. The members are the node level, the new level after processing, the parent node id and a pointer to an auxiliary data structure, from which a number of different attributes can be computed during a pass through the tree.

Max-Trees can utilize mask images to control the connectivity of the image domain. This is referred to as the *dual input Max-Tree* algorithm (Ouzounis,2007) and examples are the clustering and contraction based connectivities, which remain to be investigated in the study of the local background of regions containing rubble.
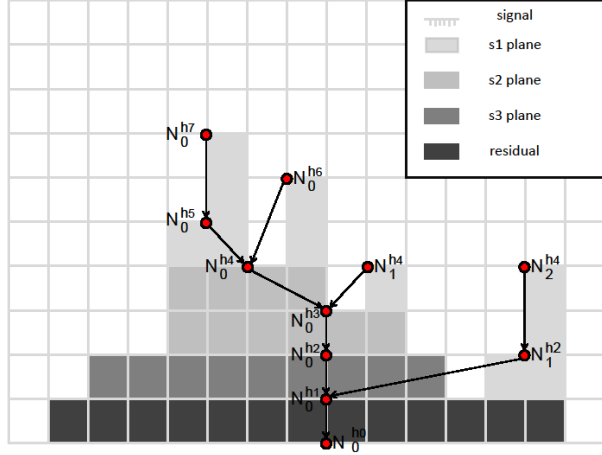
---

* Corresponding author.

Figure 1. A simple 1D signal (shaded) decomposed to 3 area zones, and the corresponding Max-Tree.

An example of a Max-Tree computed from a simple 7-level 1D signal is shown in Figure 1. A node exists for each peak component that is partially or fully a flat zone.

2.3 Image Information Mining

Projecting the input image to a tree-based structure compresses the information content by organizing same intensity path-connected elements to hierarchically ordered components that are represented by nodes. Mining the tree is a simple pass through the structure in which node attributes are compared against a given set of thresholds. In the case of rubble, size is the predominant attribute but others, like compactness, may also contribute for a more constrained representation. To constrain the search space in the mining process, the tree structure is partitioned to a set of semantic layers. A typical set-up involves a 4-layer decomposition; the noise, the rubble, the local background and the image residual layer. The decomposition algorithm employed is a third generation Differential Morphological Profile (DMP) (Pesaresi,2001), i.e. one that supports connected attribute filters (Breen,1996) for computing the contribution of each image element to the respective set of layers. The size metric in this case is the component area as opposed to width in regular DMPs. This is described as the Differential Area Profile (DAP) (Ouzounis,2010).

Let E be the definition domain of an image f. Moreover, let $\gamma_\lambda^\alpha(f)$ and $\phi_\lambda^\alpha(f)$ be an area opening and closing of f respectively (Vincent,1993). They are both connected operators, i.e. they transform the image partition of flat zones from fine to coarse (Salembier,1998); subject to an area criterion. An area opening reduces the intensity of a peak component P marked by $x \in E$ to that of its highest ancestor P' satisfying the area criterion, i.e. $\lambda \leq Area(P')$. An area closing is the dual operator.

Openings are utilized for accessing and processing bright image components and closings for dark components. Consider a top-hat and bottom-hat scale space of f based on area openings and closings respectively. The DAP of a point $x \in E$, is the concatenation of two vectors, perpendicular to the image plane, and in opposite direction with respect to each other. They are called the differential area opening and closing profiles of x, each consisting of $(I-1)$ elements, in which I is the number of scales.

(a)

(b)   (c)
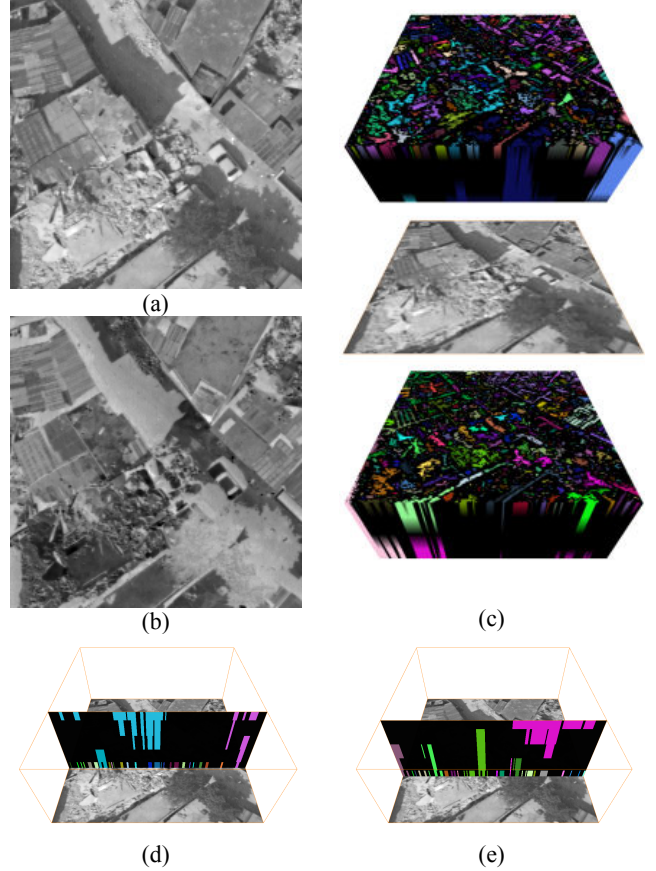
(d)   (e)

Figure 2. An image tile containing building rubble (a), and its inverse in (b). The opening (top) and closing instance (bottom) of the DAP vector field in (c). Cross sections of the two instances in (d) and (e) respectively.

The differential area opening profile of x is given by:

$$\Delta^\Pi(\gamma_\lambda^\alpha(f))(x) = \left((\gamma_{\lambda_{i-1}}^\alpha(f) - \gamma_{\lambda_i}^\alpha(f))(x) \mid \lambda_i > \lambda_{i-1}, \forall i \in [1,...,I-1]\right) \quad (1)$$

Moreover, $\gamma_{\lambda_0}^a(f) = f$. The differential area closing profile $\Delta^\Pi(\phi_\lambda^\alpha(f))(x)$ is defined analogously. Denoting vector concatenation by $\coprod$, the DAP of x is given by:

$$DAP(x) = \Delta^\Pi(\gamma_\lambda^\alpha(f))(x) \coprod \Delta^\Pi(\phi_\lambda^\alpha(f))(x). \quad (2)$$

The set of DAPs for the entire definition domain of the input image is called the DAP *vector field* and is divided into its two constituent parts, the *opening* and *closing instance*. An axial cross-section of any of the two instances is referred to as a DAP *plane*. An example is given in Figure 2. Image (a) shows the input and (b) its inverted replica. Computing the dual of a connected filter is identical to computing the original operator on the inverted image.

Image (c) shows the color labeled DAP vector field of (a). Images (d) and (e) show two sagittal cross-sections, of the opening and closing instance of the DAP vector field respectively. The bottom-most plane of each instance contains all small size components. Planes are also referred to as *area zones* because they contain objects of strict size limits. The gray shaded bands of the signal in Figure 1 demonstrate a 4-area zone partition of the input signal; the (1,4), (4,8), (8,10) and (10, *image size*) zone respectively. The area zone decomposition of the input images of Figure 2, i.e. (a) and (b), considers the first plane of each instance to contain all rubble candidates. There is no noise layer due to resolution limitations. Following fine tuning of the area zone thresholds, discussed in Section 3, the rubble layer is computed by summing the two primary zones/planes of the respective instances.

2.4 Information Meta-Process

The extracted rubble layer following an area-based tree query is an image consisting of rather low intensity components that correspond to image features, both dark and bright, of size within the corresponding area zone bounds. They convey geometric and intensity information that can be perceived as low level semantics. Shape is not considered in our approach. Intensity specifies the extent to which each component stands out with respect the local background layer. Bright components in the rubble layer however, do not necessarily correspond to rubble. To suppress the response of such cases, the spatial distribution of the extracted components is taken into consideration. This is through a commonly used method in cluster analysis; the spatial aggregation. This yields a set of higher level semantics considering the density metric; the rubble clusters. Spatial aggregation is a spatial averaging of a gray-level function over a finite neighborhood. Assuming a Gaussian distribution of standard deviation σ, the process reduces to low a pass filter or Gaussian blur, given by:

$$G(x) = \frac{1}{\sqrt{2\pi\sigma^2}} e^{-\frac{x^2}{2\sigma^2}}. \qquad (3)$$

I.e. given a point $x \in E$ defining the centre of a Gaussian kernel K, its intensity is given by averaging the weighted intensities of its neighbors within K. $G(x)$ is the value of the density metric at x.

3. RD SYSTEM OPERATION CYCLE

3.1 System Input

In this section a rubble detection exercise is demonstrated on a limited coverage dataset. The process flow initiates at the image representation stage and no pre-processing or additional input sources are used. This is done to highlight the strength of the proposed methodology directly on the raw, primary source. The dataset used is a set of VHR aerial images of Port-au-Prince after the Haiti earthquake in January 12th, 2010. They are courtesy of ©Google 2010, and are available at the Google Crisis Response web-site (Google,2010). They are sub-sampled to 8-bits/pixel.

3.2 Interactive Image Decomposition and Query

In the first stage of the process flow, the primary input is projected onto a Max-Tree and a Min-Tree structure for bright and dark information indexing respectively. A Min-Tree is the dual of a Max-Tree. Instead of involving a separate algorithm to compute it,
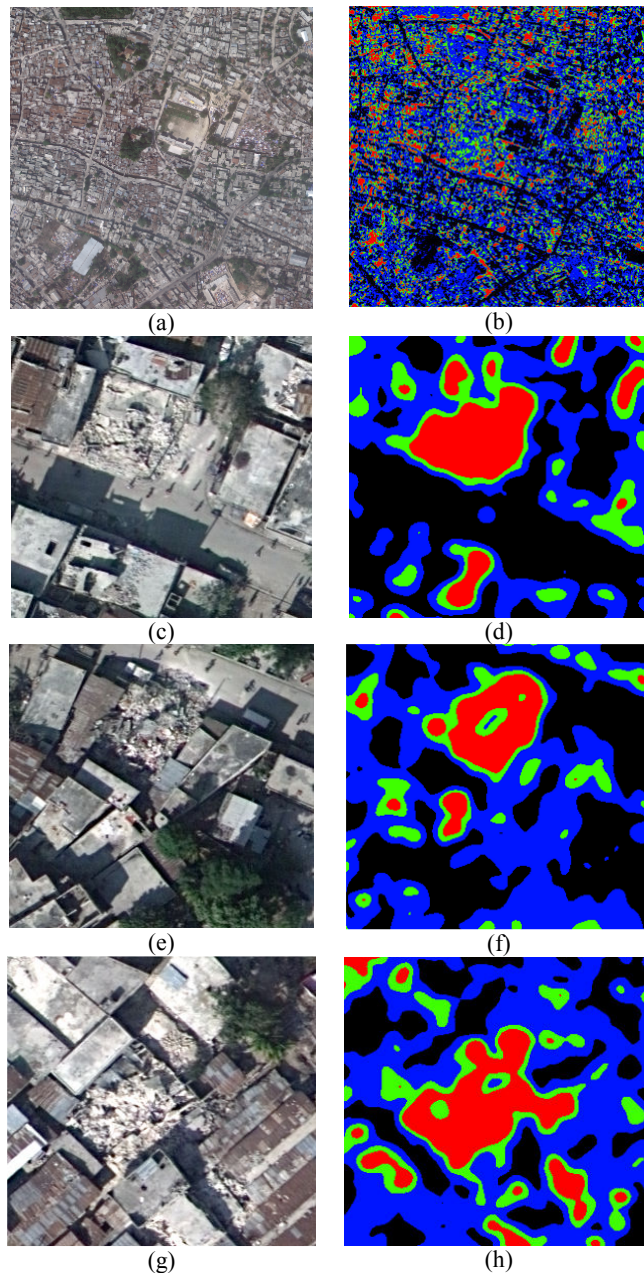

Figure 3. An RGB tile of Port-au-Prince aerial imagery dataset in (a) and the detected rubble clusters in (b). Images (c)-(h) show selected regions of (a) and (b) respectively.

it is sufficient to invert the input image and re-compute the Max-Tree. Computing the two trees is a rather intensive task for which the RD system employs a concurrent implementation of the algorithm, for shared memory, multi-processor machines (Wilkinson,2008). It has been utilized for computing regular DMPs in (Wilkinson,2011). In the case of DAPs, following the concurrent tree construction, it runs the area zone decomposition algorithm of (Ouzounis2011a). In this algorithm the tree is partitioned into sets of nodes based on their size attributes; each set contains all the tree nodes that correspond to image features with size being within the zone's bounds. This process is

implemented in the form of a top-down pass through the tree and its runtime is independent of the number of zones. Moreover, zones can be split or merged interactively thus allowing for fine tuning of the decomposition, i.e. selecting the optimal thresholds to define the rubble layer. The thresholds are selected after examining several manually identified regions containing rubble.

Rubble in the given exercise can be approximated by 5-pixel wide square tiles. The spatial resolution of the input image is 0.139m/pixel, thus rubble chunks are of estimated size up to 0.7m. The minimum building height of regular houses including the roof, in normal residential areas, i.e. excluding slums, commercial districts, etc., is estimated to 3.5m. If a wall collapses the debris is expected to reach a distance equal to twice its height from the corresponding footprint edge, i.e. approximately 7m. This is called the *rubble expectation radius R,* and the ratio of *R* to rubble width is used empirically as a generalization scale for specifying the size of the Gaussian kernel. In this case the ratio equals 10, which multiplied by the rubble width in pixels, yields 50 elements associated to each reference point, i.e. a 51-element wide kernel.

The operation cycle was tested on a set of 75 square tiles, each being 4096-element wide and of 8-bit intensity resolution. The set was processed as a single image of total size of 1.2GB. A 20-scale size decomposition was computed with the bounds of the first plane/zone of each of the two instances of the DAP vector field set to (1,25). The remaining 18 planes did not contribute to the overall rubble analysis but were purposely set to add redundancy to the system. The rubble detection cycle (image representation and decomposition) was computed in 194.16s. on a 24 core Opteron-based machine (4-socket 6 cores per socket) with 128GB of memory, when using 24 threads.

4. INTERPRETATION AND QUALITY ASSESMENT

Figure 3 shows the results of cluster analysis, i.e. the higher level semantics. Image (a) shows an original tile and (b) shows the detected rubble clusters. The colour code is from blue to red (or dark to bright), i.e. low to high density and is computed on the rubble layer following histogram stretching. Images (c) – (h) show selected regions of the original (left) and the corresponding rubble clusters (right). The quality of the results was assessed by visual inspection, following a density threshold on the cluster image that was set empirically to the mid-range value. For the tile in Image (a), the method detected 92 correct targets and 5 false alarms (3 dump sites and 2 corrugated roofs). Moreover, 2 targets were missed.

5. CONCLUSIONS

The proposed method was tested for the case of a simple dichotomy, i.e. detecting rubble against the global background. The detection success rate for the tile of Figure 3 was approximately 92%, suggesting that the method in its simplest form is sufficiently reliable for rapid damage assessment. In future work, we aim at utilizing the local background information layer to minimise the false alarms. Richer set of constraints, based on attribute vectors, are investigated for computing more delicate decompositions. Moreover, an automatic assessment method is being developed to compare the results of our method against the ground truth (JRC,2010) in a full scale exercise on the entire Port-au-Prince dataset (360GB), currently under preparation.

REFERENCES

References from Journals and Conference Proceedings

E.J. Breen, and R. Jones, "Attribute openings, thinnings and granulometries", Comp. Vision and Image Understanding, vol. 64(3), p.p. 377-389, 1996.

G.K. Ouzounis, and M.H.F. Wilkinson, "Mask-based second-generation connectivity and attribute filters", IEEE Tran. Pattern Analysis and Machine Intell., vol. 29(6), p.p. 990-1004, 2007.

G.K. Ouzounis, and P. Soille, "Differential area profiles", Proc. 20th Int. Conf. Pattern Recognition (ICPR), Istanbul, p.p. 4085-4088, Aug. 2010.

G. K. Ouzounis, M. Pesaresi, and P. Soille, "Differential area profiles: properties and efficient computation", IEEE Tran. Pattern Analysis and Machine Intelligence, 2011, (submitted).

G. K. Ouzounis, and P. Soille, "Attribute constrained connectivity and the Alpha-Tree representation", IEEE Tran. Image Processing, 2011, (submitted).

M. Pesaresi, and J.A. Benediktsson, "A new approach for the morphological segmentation of high-resolution satellite imagery", IEEE Tran. Geoscience and Remote Sensing, vol. 39(2), p.p. 309-320, 2001.

P. Salembier, A. Oliveras, and L. Garido, "Anti-extensive connected operators for image and sequence processing", IEEE Tran. Image Processing, vol. 7(4), p.p. 555-570, 1998.

L. Vincent, "Morphological area openings and closings for gray-scale images", Shape in picture: math. description of shape in grey-level images, NATO, p.p 197-208, 1993.

M.H.F. Wilkinson, H.Gao, W.H. Hesselink, J. E. Jonker, and A. Meijster, "Concurrent computation of attribute filters using shared memory parallel machines", IEEE Tran. Pattern Analysis and Machine Intell., vol. 30(10), p.p. 1800-1813, 2008.

M.H.F. Wilkinson, P. Soille, M. Pesaresi, and G.K. Ouzounis, "Concurrent computation of differential morphological profiles on giga-pixel images", Proc. 10th Int. Symp Mathematical Morphology (ISMM 2011), Intra, July 2011, (submitted).

References from Websites

Google, 2010. Google Crisis Response, "Haiti Earthquake – Imagery Download", http://www.google. com/relief/ haitiearthquake/imagery.html

JRC,2010. JRC Response To Emergencies And Disasters, "Haiti Earthquake", http://lunar.jrc.it/disasters/Crisis/HaitiEarthquake/ tabid/425/Default.aspx